Salmonella typhimurium and *Escherichia coli* Dissimilarity: Closely Related Bacteria with Distinct Metabolic Profiles

Cintia R. Sargo, Gilson Campani, Gabriel G. Silva, Roberto C. Giordano, Adilson J. Da Silva, and Teresa C. Zangirolami

Graduate Program of Chemical Engineering, Federal University of São Carlos, Rodovia Washington Luís, Km 235, São Carlos, SP 13565-905, Brazil

Daniela M. Correia

Graduate Program of Chemical Engineering, Federal University of São Carlos, Rodovia Washington Luís, Km 235, São Carlos, SP 13565-905, Brazil

CEB—Centre of Biological Engineering, University of Minho, Campus De Gualtar, Braga 4710-057, Portugal

Eugénio C. Ferreira and Isabel Rocha

CEB—Centre of Biological Engineering, University of Minho, Campus De Gualtar, Braga 4710-057, Portugal

DOI 10.1002/btpr.2128
Published online July 3, 2015 in Wiley Online Library (wileyonlinelibrary.com)

Live attenuated strains of Salmonella typhimurium have been extensively investigated as vaccines for a number of infectious diseases. However, there is still little information available concerning aspects of their metabolism. S. typhimurium and Escherichia coli show a high degree of similarity in terms of their genome contents and metabolic networks. However, this work presents experimental evidence showing that significant differences exist in their abilities to direct carbon fluxes to biomass and energy production. It is important to study the metabolism of Salmonella to elucidate the formation of acetate and other metabolites involved in optimizing the production of biomass, essential for the development of recombinant vaccines. The metabolism of Salmonella under aerobic conditions was assessed using continuous cultures performed at dilution rates ranging from 0.1 to 0.67 h^{-1}, with glucose as main substrate. Acetate assimilation and glucose metabolism under anaerobic conditions were also investigated using batch cultures. Chemostat cultivations showed deviation of carbon towards acetate formation, starting at dilution rates above 0.1 h^{-1}. This differed from previous findings for E. coli, where acetate accumulation was only detected at dilution rates exceeding 0.4 h^{-1}, and was due to the lower rate of acetate assimilation by S. typhimurium under aerobic conditions. Under anaerobic conditions, both microorganisms mainly produced ethanol, acetate, and formate. A genome-scale metabolic model, reconstructed for Salmonella based on an E. coli model, provided a poor description of the mixed fermentation pattern observed during Salmonella cultures, reinforcing the different patterns of carbon utilization exhibited by these closely related bacteria. © 2015 American Institute of Chemical Engineers *Biotechnol. Prog.*, 31:1217–1225, 2015
Keywords: Salmonella typhimurium, aerobic/anaerobic conditions, extracellular metabolomics

Introduction

Salmonella is a rod-shaped, Gram-negative, facultatively anaerobic, flagellated bacterium that belongs to the *Enterobacteriaceae* family, of which *Escherichia coli*, *Shigella*, and *Klebsiella pneumonia* are also members.[1]

Salmonella enterica serovar Typhimurium (*S. typhimurium*) is an important intracellular pathogen, causing acute gastroenteritis in humans and many other mammalian species.[2,3] However, attenuated strains of this bacterium have been investigated to develop several biotechnological products.[4] Amongst these products, promising results have been obtained for potential vaccine delivery systems for foreign antigens against a diversity of infectious agents, including bacteria (such as *Helicobacter pylori, Salmonella enterica* serotype Typhi and *Streptococcus pneumoniae*), viruses (HIV and influenza), parasitic pathogens, and cancer.[5–9] Hence, *S. typhimurium* is a microorganism with significance in both medicine and biotechnology, and has been studied extensively in the areas of genetics[10] and immunology.[4,11,12] In last years, several studies have been published regarding *S. enterica* metabolism regulation.[13–17] However, there is still little information available concerning the metabolic aspects of its growth under different conditions, which are essential to understand its metabolism and improve biotechnological processes.

Escherichia coli is the most studied and best characterized microorganism in terms of genome annotation, biochemical

Additional Supporting Information may be found in the online version of this article.

Correspondence concerning this article should be addressed to T. C. Zangirolami at teresacz@ufscar.br.

genetics, molecular biology, and growth behavior, and is one of the first organisms to have had the complete genome sequenced.[18] Studies of its metabolism have demonstrated that *E. coli* cells produce acetate as an extracellular byproduct under aerobic conditions, and that the organism is also able to metabolize this acetate as sole carbon and energy source.[19–23] In the absence of oxygen, the cells produce a mixture of organic acids (formic, lactic, succinic, and acetic) and ethanol.[24,25]

The production of acetate by *E. coli* strains has been extensively studied over the past few decades[26–28] and is highly relevant for bioprocesses, because this byproduct decreases cellular growth, even at concentrations as low as 0.5 g L^{-1}, and inhibits the synthesis of recombinant proteins.[20,29–31] This overflow phenomenon occurs at high glucose uptake rates and, according to Vemuri et al.,[27] has been attributed to an enzymatic limitation in the TCA cycle, whereby the carbon flux from acetyl-CoA is directed to acetate via acetyl phosphate, instead of entering the TCA cycle.

It is widely known that *E. coli* K12 is the closest bacterial species to *Salmonella*, sharing about 85% of the genome of the latter.[32,33] The main differences between these organisms are related to virulence factors, because *E. coli* K12 is not pathogenic, unlike *Salmonella*. According to Götz et al.,[34] the two microorganisms have similar metabolic settings, including all the genes for the major central metabolic pathways.

Wilson et al.[35] described the stoichiometry of *Salmonella typhimurium* LT2 growth in batch cultures carried out with complex medium, at different initial pH values. This study reported that acetic acid was the predominant organic acid produced.

A better knowledge of *S. typhimurium* metabolism and its extracellular metabolite production profile is required to develop protocols for growing these cells at high density and improve bioprocesses for the large scale production of vaccines and biopharmaceutical products. This kind of study has already been reported for other microorganisms such as *Escherichia coli*, *Bacillus subtilis*, and *Mannheimia haemolytica*, based on combinations of steady-state culture data and stoichiometric metabolic models.[36–38]

Studies of the cellular metabolism of many organisms can now be assisted by bioinformatics tools, which combine *in silico* genome-scale reconstruction of metabolic reaction networks with mathematical modeling approaches, such as flux balance analysis (FBA), employing tools such as Optflux.[39] According to Raman and Chandra,[40] these tools enable prediction of the growth rates of organisms and their substrate uptake rates, as well as the rates of production of biotechnologically relevant metabolites, and are important for optimization of industrial bioprocesses. Examples of applications of FBA include maximization of the production of organic acids, polysaccharides, amino acids, and industrial solvents (such as acetone and butanol production by *Clostridium acetobutylicum*[41,42]), as well as the identification of potential drug targets (for example, the identification of targets for anti-tubercular drugs designed by systematically deleting genes *in silico*[43]), and the analysis of metabolic networks for microorganisms such as *Corynebacterium glutamicum*[44] and *E. coli*.[45]

The aim of this work was to evaluate the metabolism of wild type *S. typhimurium* under aerobic (with glucose or acetate as carbon source) and anaerobic conditions. Predictions obtained with the genome-scale STM_v1.0 metabolic model reconstructed for *S. typhimurium* by Thiele et al.,[46] as well as experimental data, were used to compare the extracellular metabolism of *Salmonella* and *E. coli*.

Materials and Methods

Bacterial strain, growth medium, and culture conditions

The strain used in the present study was *S. typhimurium* LT2 obtained from the Salmonella Genetic Stock Centre (University of Calgary, Canada).

Pre-cultivations of all experiments were conducted in 2YT medium (16 g tryptone, 10 g yeast extract, and 5 g NaCl per liter), and glucose-limited medium (M9 minimum medium) contained (per liter): 7.53 g $Na_2HPO_4{\cdot}2H_2O$; 3 g KH_2PO_4; 1 g NH_4Cl; and 0.5 g NaCl. The following components were filter sterilized and then added to the medium: 0.11 g $MgSO_4{\cdot}6H_2O$; 0.34 g thiamine; 0.015 g $CaCl_2$; 2 mL of trace vitamin solution; and 2 mL of trace minerals solution. The composition of the trace vitamin solution was (per liter): 0.42 g riboflavin; 6.1 g nicotinic acid; 5.4 g pantothenic acid; 1.4 g pyridoxine; 0.06 g biotin; and 0.04 g folic acid. The composition of the trace minerals solution was (per liter): 27 g $FeCl_3$; 2 g $ZnCl_2$; 2 g $CoCl_2$; 2 g $NaMoO_4$; 1 g $CaCl_2$; 1 g $CuCl_2$; 0.5 g H_3BO_3; and 100 mL HCl. Glucose was used as the carbon source in aerobic continuous cultivations (10 g L^{-1}) and anaerobic batch cultivations (15 g L^{-1}). In addition, aerobic batch culture was also carried out using acetate (5.5 g L^{-1}).

Aerobic culture with glucose as carbon source

Aerobic continuous cultivations were conducted at 37°C in a 2 L a stirred tank bioreactor (Applikon, Netherlands) with a working volume of 800 mL. The pH was controlled at 7.0 by automatic addition of NH_4OH (5%, v/v).

In these experiments, two stages of inoculum preparation were performed in flasks. A single colony from a 2YT agar plate was suspended in 10 mL of 2YT medium and, after growing at 200 rpm and 37°C to an optical density at 600 nm (OD_{600nm}) of approximately 2.0 (exponential growth phase), 1 mL of cell suspension was transferred to a flask containing 80 mL of M9 minimal medium. The second culture was grown until OD_{600nm}= 2.0 and then inoculated into the reactor to obtain an initial OD_{600nm} of 0.2.

The M9 minimal medium was continuously fed to the bioreactor at dilution rates (D) of 0.10 (±0.01), 0.15 (±0.01), 0.24 (±0.02), 0.48 (±0.03), 0.58 (±0.04), and 0.67 (± 0.04) h^{-1}. Changes in D were implemented by altering the flow rate of fresh medium into the bioreactor. An agitation speed of 800 rpm and a constant air flow rate (from 0.8 to 1.5 SLPM, depending on the dilution rate), controlled by a mass flow controller, ensured that dissolved oxygen concentrations remained well above 20% of saturation. The exhaust gas composition was analyzed using a Sick/Maihak S.710 analyzer, and data were monitored with a cFP controller (National Instruments).

The steady state was inferred after measuring the optical density and the concentrations of dissolved oxygen and carbon dioxide in the bioreactor, and was considered to have been reached when these variables remained constant for at least three residence times. On-line data acquisition and automatic pH control employed SuperSys_HCDC software.[47,48]

Aerobic culture with acetate as carbon source

Aerobic batch culture with acetate minimal medium was performed at 37°C in a 2 L stirred tank bioreactor (Applikon, Netherlands) with a working volume of 1.6 L. The pH was controlled at 7.0 by automatic addition of NH_4OH (5%, v/v) and H_2PO_4 (21%, v/v), and data were acquired online.

In this experiment, inoculum preparation was carried out in three stages. The first two were the same as described above for the aerobic culture with glucose as carbon source. Subsequently, a batch culture with 10 g L^{-1} of glucose was conducted to obtain a cellular concentration of ~1.8 g_{DCW} L^{-1}. The final cell suspension was aseptically removed from the reactor and centrifuged. The resulting pellets were resuspended in 1.6 L of M9 minimal fresh medium containing acetate as carbon source. The new suspension was transferred back to the bioreactor and the cultivation was started.

The dissolved oxygen concentration was monitored and maintained at 20% by a controller that automatically adjusted the agitation speed (between 200 and 800 rpm) and the air flow rate (between 0.3 and 0.6 SLPM), using the SuperSys_HCDC software.

Anaerobic culture

The inoculum for anaerobic batch cultivation was prepared as described for the aerobic culture with glucose as carbon source. The centrifuged biomass was resuspended in 1.6 L of M9 minimal fresh medium containing 15 g L^{-1} of glucose as sole carbon source. The new suspension was transferred back to the 2 L bioreactor (Applikon, Netherlands) and an intense flow of industrial N_2 (0.6 SLPM) was applied to quickly remove traces of dissolved O_2. Anaerobic conditions were maintained by supplying a constant stream of ultra-pure N_2 at a flow rate of 0.3 SLPM. The pH, temperature, and agitation rate were kept at 7.0, 37°C, and 300 rpm, respectively. Anaerobic conditions in the bioreactor were monitored by measuring the O_2 content in the exhaust gas using a Sick/Maihak S.710 analyzer. Only data collected at 0% O_2 mole fraction were used to characterize anaerobic metabolism.

Analytical methods

Cellular growth was followed by measuring the optical density of the culture broth at a wavelength of 600 nm (OD_{600nm}) and by determining the dry cell weight (DCW). For dry cell weight, a known volume of culture broth was filtered using pre-weighed 0.22 μm cellulose-nitrate membranes (UNIFIL) and dried to a constant weight at 90°C for 24 h. The biomass concentration (C_x) was estimated from the OD measurements and dry cell weight data obtained in all experiments by linear regression (Eqs. 1 or 2).

$$C_x(\mathrm{g/L}) = 0.39 \pm 0.01^{*}\mathrm{OD}_{600}\ (\text{experiments with glucose as carbon source}) \quad (1)$$

$$C_x(\mathrm{g/L}) = 0.36 \pm 0.01^{*}\mathrm{OD}_{600}\ (\text{experiment with acetate as carbon source}) \quad (2)$$

Samples of culture medium were centrifuged at 10,000 rpm and 4°C for 5 min and the supernatants were further filtered through a 0.2 μm PVDF membrane (GVS) and stored at −20°C until further analysis.

The concentrations of glucose and extracellular metabolites (acetate, formate, ethanol, succinate, lactate, among others from Sigma-Aldrich organic acid kit, as well as pyruvate) were determined by HPLC (Waters Corp. system), using an Aminex HPX-87H column (Bio-Rad) and 5 mM sulfuric acid solution as the mobile phase (at a flow rate of 0.6 mL/min). The column temperature was 60°C. Organic acids were detected at 210 nm (Waters 486 UV detector), while glucose and ethanol were measured with a refractive index detector (Waters 410). Glucose was also determined enzymatically using a glucose oxidase assay (GOD-PAP, Laborlab, Brazil), according to the manufacturer's instruction.

Flux calculations

For all chemostat or batch experiments, fluxes were estimated using Eq. 3:[49]

$$J_i = \frac{r_i}{C_x} \quad (3)$$

where J_i is the consumption or production flux of component i (substrate, metabolic products, oxygen, or carbon dioxide), in mmol $g_{DCW}{}^{-1}$ h^{-1}; r_i is the volumetric rate of consumption or production of component i, in mmol L^{-1} h^{-1}; and C_x is the biomass concentration (g_{DCW} L^{-1}). From the material balance for a continuous, steady-state bioreactor, with no biomass in the feed stream, the volumetric rates were assessed from the measured concentrations of biomass, glucose (C_S, at the inlet and outlet), and organic acids, according to Eqs. 4–6:

$$r_S = \frac{D \cdot \left(C_S^{in} - C_S^{out}\right)}{MM_S} \quad (4)$$

$$r_P = \frac{D \cdot C_P^{out}}{MM_P} \quad (5)$$

$$r_X = \mu \cdot C_X = D \cdot C_X \quad (6)$$

where D is the dilution rate (h^{-1}), C_S^{in} is the substrate concentration in the feed medium, C_S^{out} and C_P^{out} are the outlet concentrations of substrate and metabolic products under steady-state conditions (g L^{-1}), MM_S and MM_P are the molecular masses of substrate and metabolic products (g $mmol^{-1}$), respectively, and μ is the specific growth rate (h^{-1}).

For both continuous and batch cultures, the rates of oxygen consumption (*OUR*) and carbon dioxide production (*CER*) were calculated from the mass balance for the gas phase, as follows:

$$\mathrm{OUR} = \left(y_{O_2}^{in} - y_{O_2}^{out}\right) \cdot \frac{Q \cdot P}{R \cdot T \cdot V_t} \quad (7)$$

and

$$\mathrm{CER} = \left(y_{CO_2}^{out} - y_{CO_2}^{in}\right) \cdot \frac{Q \cdot P}{R \cdot T \cdot V_t} \quad (8)$$

where $y_{O_2}^{in}$ and $y_{CO_2}^{in}$ are the mole fractions of oxygen and carbon dioxide, respectively, in the inlet air; $y_{O_2}^{out}$ and $y_{CO_2}^{out}$ are the mole fractions of oxygen and carbon dioxide, respectively, in the outlet gas; Q is the total gas flow rate (L h^{-1}); P and T are the pressure (atm) and temperature (K), respectively, under STP conditions; R is the molar gas constant (8.2×10^{-5} atm L $mmol^{-1}$ K^{-1}); and V_t is the working volume of the bioreactor (L).

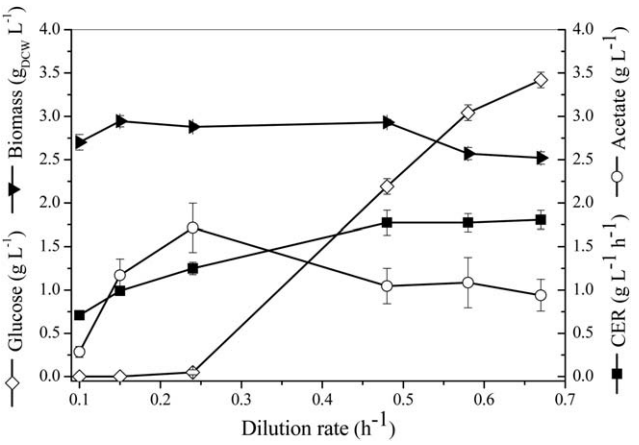

Figure 1. Growth and fermentation product profiles of *S. typhimurium* LT-2 during aerobic glucose-limited chemostat cultivations under different dilution rates.

CER (■), glucose (◇), biomass (C_x) (▶) and acetate (○). The error bars represent standard deviations from three technical replicates.

Experimental fluxes for the batch cultures were also calculated with Eq. 3, using material balances for a batch bioreactor to estimate the volumetric rates of biomass production, organic acid formation, and substrate consumption, as described by Eqs. 9–11:

$$r_S = -\frac{1}{MM_S}\frac{d(m_S/V)}{dt} \tag{9}$$

$$r_P = \frac{1}{MM_P}\frac{d(m_P/V)}{dt} \tag{10}$$

$$r_X = \frac{d(m_X/V)}{dt} \tag{11}$$

where $\frac{d(m_i/V)}{dt}$ is the slope of the curve describing the variation with time of the substrate, product, or biomass experimental mass values divided by the updated bioreactor volume.[45] Only data from the exponential growth phase were used for the volumetric rate estimates. In addition, since little biomass formation was observed during the period for which data were collected, an average value of C_x was used in Eq. 3. The biomass yield ($Y_{X/S}$) was also calculated using the exponential phase experimental data, according to Eq. 12[50]:

$$Y_{X/S} = \frac{C_X - C_{Xin}}{C_{Sin} - C_S} \tag{12}$$

where C_{Xin} and C_{Sin} refer to the biomass and substrate concentrations, respectively, at the beginning of the exponential growth phase.

In silico analysis

In silico experiments were carried out using the genome-scale STM_v1.0 metabolic model reconstructed for *S. typhimurium* by Thiele et al.,[46] to simulate the metabolic profile of this bacterium under different environmental conditions. The metabolic network described by the model consists of 1,270 genes; 2,201 intracellular reactions; 345 exchange reactions; and 1,119 metabolites.

Simulations were run with the Optflux v. 3.2.1 open-source software platform (www.optflux.org), using the parsimonious flux-balance analysis (pFBA) method, with biomass maximization as the objective function.[51] The results of these simulations were compared with the experimental data obtained from the *in vitro* experiments.

Results and Discussion

S. typhimurium vs. *E. coli* aerobic metabolism

Chemostat experiments with *Salmonella typhimurium* were performed under aerobic conditions with dilution rates (D) ranging from 0.1 to 0.7 h^{-1}, and the results were used to map the formation of metabolites (data presented in Supporting Information Figure S1).

The concentrations of biomass, residual glucose, and byproducts, and the CO_2 evolution rate (CER), were plotted as a function of D (Figure 1). At lower dilution rates (between 0.1 and 0.24 h^{-1}), it was observed that the cells consumed all the glucose provided, and that the carbon dioxide evolution increased linearly with the dilution. It was also possible to observe carbon deviation towards byproduct formation by the *S. typhimurium* cells, with acetate as the only metabolite produced. At dilution rates of 0.48 h^{-1} and above, glucose uptake slowed down (Figure 3A) and a considerable increase of the residual glucose concentration was observed. Consequently, the concentrations of acetate and biomass decreased due to washout effect. Formate at low concentrations (< 0.5 g L^{-1}) was also detected at dilution rates above 0.48 h^{-1}. The formation of this metabolite is probably related to cell lysis and release of DNA, which can act as barrier, hampering oxygen diffusion into the cells[52] (data presented in Supporting Information Figure S2).

All data obtained under steady-state conditions were tested for consistency by applying mass balances. The distribution of carbon towards biomass, carbon dioxide and acetate during steady-state growth, estimated from the mass balance results, are shown in Figure 2A.

Carbon recovery ranges from 94 to 106%, which demonstrates the consistency of the experimental data obtained for the chemostat cultures. It was observed that for *Salmonella*, in most cases, from 11 to 17% of the carbon source was directed towards the production of organic acids (except at a dilution rate of 0.1 h^{-1}).

Kayser et al.[37] and Brown et al.[53] reported that acetate overflow occurs at higher dilution rates in continuous cultures of *E. coli*. In these studies, pronounced acetate production was observed for D above 0.4 and 0.5 h^{-1}, respectively, both close to the washout point, when the concentrations of residual glucose and acetate increased considerably, concomitant with reductions in the biomass concentration and CO_2 production (Figure 2B). Different behavior was observed in the present work for the continuous cultures of *S. typhimurium*. A better understanding of these differences could be obtained from a comparison of acetate metabolism in *E. coli* and *S. typhimurium*, as described below.

S. typhimurium vs. *E. coli* acetate metabolism

Batch cultivation with acetate minimal medium was performed to evaluate acetate assimilation by *S. typhimurium* under aerobic conditions and compare it to *E. coli* metabolism. According to Raghunathan et al.,[54] both microorganisms can grow in acetate as sole carbon source, as supported by the results shown in Table 1.

In *E. coli* and *Salmonella*, the metabolism of acetate as sole carbon and energy source involves two steps. Acetate is first transported into the cell and subsequently activated to

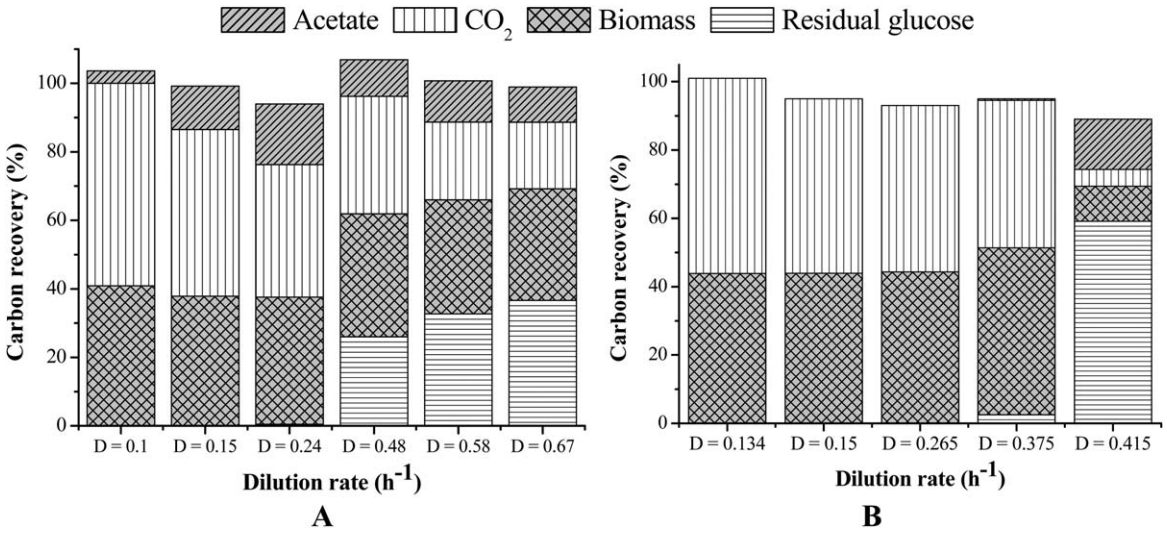

Figure 2. Influence of specific growth rate on the carbon distribution in aerobic glucose-limited chemostats at different dilution rates for (A) wild-type *S. typhimurium* LT-2 and (B) *E. coli* K-12 TG1 (data from Kayser et al.).[37]

acetyl-CoA, and is then metabolized in the tricarboxylic acid cycle and glyoxylate shunt.[22,55] There are two distinct pathways responsible for the acetate activation: Ack-Pta (acetate kinase - EC 2.7.2.1 and phosphotransacetylase—EC 2.3.1.8), where acetate is activated by means of an acetyl phosphate intermediate, or Acs (acetyl coenzyme A synthetase—EC 2.7.2.1).[56] For *S. typhimurium* there is little information about the activity of enzymes involved in production/assimilation of acetate. According to Starai et al.,[15] the acetate assimilation is associated with Acs and Ack-Pta enzymes when ethanolamine is used as carbon source. In contrast, for *E. coli*, there is a considerable number of studies about acetate uptake.[19,22,56,57] Despite the conflicting views presented by these works, in general, it is accepted that Ack-Pta and Acs pathways play a role on acetate assimilation.

During the cultivation, a long lag phase (almost 15 h) was observed, which demonstrates the difficulty experienced by *Salmonella* cells in shifting from glucose to acetate metabolism. Glucose catabolite repression was extensively study for *E. coli*, that can need more than 3 h to start to grow in a new substrate.[22,58–60] So far, studies addressing glucose repression on Salmonella have not been reported.

Comparison of the growth rates achieved on acetate showed that the *Salmonella* growth rate was slower than reported for different *E. coli* strains (Table 1). The biomass yields under this condition were similar for the two microorganisms. However, the main difference between the bacteria was the acetate uptake rate, which was 3-fold lower for *Salmonella* cells. The inferior performance on acetate exhibited by *Salmonella* is probably related to a lower activity of Ack-Pta or Acs enzymes than in *E. coli* cells, which can be assessed by comparing K_m values for both bacteria. The affinity of AckA for acetate as substrate in *S. typhimurium* is lower or equal ($K_m = 1.2$ mM[61] or 7 mM[62]) than the observed for *E. coli* ($K_m = 7$ mM).[62] On the other hand, Acs of *E. coli* K12 binds with much higher affinity ($K_m = 0.2$ mM)[63,64] than the Acs of *S. typhimurium* LT-2 ($K_m = 40$[65] or 6 mM[66]) .[53,54] It is important to highlight that the mentioned K_m values were obtained using different pH conditions.

Therefore, although *Salmonella* is able to assimilate acetate, the process occurs at a low rate. For this reason, during the *Salmonella* chemostat cultures, net acetate production was observed for all the dilution rates tested (Figure 2A), which was not the case for *E. coli* (Figure 2B), due to its more efficient acetate uptake system.

S. typhimurium vs. *E. coli* anaerobic metabolism

According to Driessen et al.,[68] the fermentation pattern of *S. typhimurium* is very similar to that observed for *E. coli*, which converts glucose into a mixture of organic acids when cultivated in the absence of O_2.

Acetate was the major by-product in the aerobic chemostat culture. However, in the anaerobic batch culture of *S. typhimurium* LT-2, besides acetate, there was significant production of ethanol and formate, with concentrations of 5.7, 7.1, and 4.3 g L^{-1}, respectively, after 3 h of cultivation. Succinate, a minor fermentation product, was also found, accounting for less than 3% of the total products formed from glucose. In the absence of oxygen, the cells converted almost all the glucose to organic acids, with low cellular growth and negligible production of CO_2.

The concentrations measured during the anaerobic batch culture of *S. typhimurium* were used together with the reactor mass balances (Eqs. 3, 9, 10, and 11) to estimate the corresponding fluxes and yield coefficients (Eq. 12). These are shown in Table 2 and Figure 4, together with comparative fluxes and biomass yield values for *E. coli*, determined from data available in the literature.[19,69]

The results indicated that the rate of glucose uptake by *Salmonella* under anaerobic conditions was about 3-fold lower than observed for *E. coli*. In addition, *Salmonella* directed less carbon towards biomass production, and the growth rate was about 4-fold lower than for *E. coli*. For both microorganisms, the main products were formate, ethanol, and acetate, but *S. typhimurium* accumulated more lactate, compared to *E. coli* strains (Figure 4).

Quantitative comparison of *in silico* and experimental data for *S. typhimurium* metabolism

In silico studies of *S. typhimurium* glucose metabolism, under both aerobic and anaerobic conditions, were performed using the genome-scale STM_v1.0 metabolic model reconstructed for *S. typhimurium*,[46] to evaluate the ability of the model to predict

Table 1. Comparison of Growth and Metabolic Parameters of *S. typhimurium* LT-2 and Different *E. coli* Strains in Batch Aerobic Cultures Using Acetate Minimal Medium

Growth Parameters	*S. typhimurium* LT-2*	*E. coli* BW2511[†]	*E. coli* B/*r*[‡]
Biomass yield (g_{DCW} g^{-1})	0.31 ± 0.09	0.26 ± 0.01	0.19 ± 0.05
Maximum growth rate (h^{-1})	0.13 ± 0.01	0.28 ± 0.03	0.30 ± 0.09
Acetate uptake rate (mmol g_{DCW}^{-1} h^{-1})	7.5 ± 1.9	24.67 ± 1.59	ND

*Deviations represent mean square error of the regressions.
[†]Data from Castaño-Cerezo et al.[19]
[‡]Data from Andersen and Meyenburg.[67]
ND: not described.

Table 2. Comparison of Growth and Metabolic Parameters of *S. typhimurium* LT-2 and Different *E. coli* Strains in Batch Anaerobic Cultures Using Glucose Minimal Medium

Growth Parameters	*S. typhimurium* LT-2*	*E. coli* BW2511[†]	*E. coli* K-12MG1655[‡]
Biomass yield (g_{DCW} g^{-1})	0.077 ± 0.007	0.1 ± 0.003	0.16 ± 0.02
Growth rate (h^{-1})	0.11 ± 0.03	0.48 ± 0.03	0.42 ± 0.01
Glucose uptake flux (mmol g_{DCW}^{-1} h^{-1})	9.6 ± 1.1	25.4 ± 0.96	14.9 ± 2.4

*Deviations represent mean square error of the regressions.
[†]Data from Castaño-Cerezo et al.[19]
[‡]Data from Chen et al.[69]

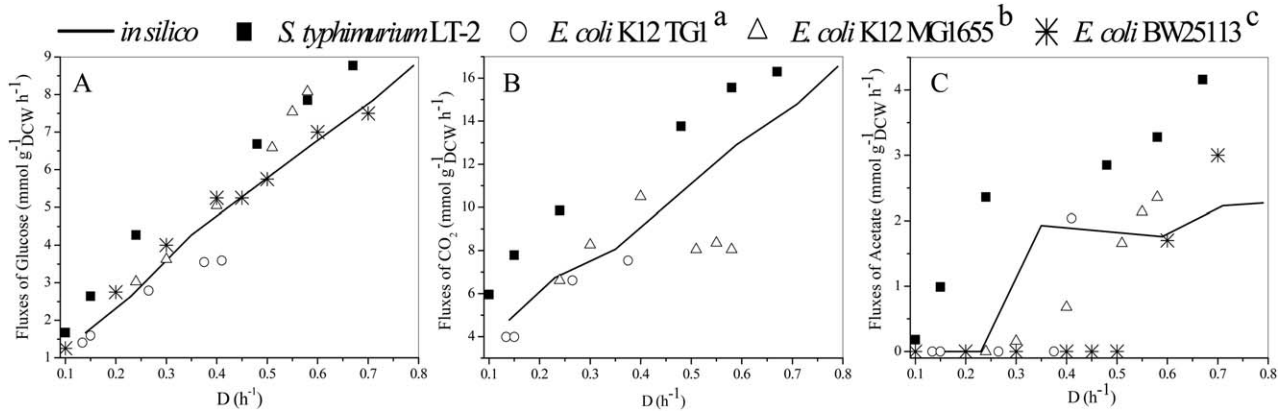

Figure 3. Comparison of fluxes of (A) glucose, (B) CO_2, and (C) acetate based on experimental data for *S. typhimurium* LT-2 (■); *E. coli* K12 TG1[a] (○); *E. coli* K12 MG1655[b] (△) and *E. coli* BW25113[c] (∗), cultivated as chemostats under aerobic conditions.

In silico solutions (—) estimated using experimental GUF and OUF values obtained in this work as the environmental conditions (Data from: [a]Kayser et al.[37]; [b]Valgepea et al.[31]; [c]Renilla et al.[26]).

the metabolism of this bacterium. This was accomplished by comparing the *in silico* results with the experimental data.

In the aerobic metabolism simulations, the glucose and oxygen uptake fluxes (GUF and OUF, respectively) were restricted to the values observed experimentally in the chemostat cultures, to determine the *in silico* flux distributions of extracellular metabolites, CO_2, and biomass under the conditions employed in the experiments (Figure 3). For comparison, chemostat data for *E. coli* cultivated under aerobic conditions[37] are also included in Figure 3, together with the simulated results using the same model.

The results obtained *in silico* were qualitatively similar to the experimental data, but the flux values showed significant differences. For all the cases studied under glucose-limited growth conditions (Figures 3A–C), the model estimated higher fluxes for biomass formation and lower fluxes for metabolite production when compared to *S. typhimurium* experimental data. The model predictions showed better agreement with the *E. coli* than the *S. typhimurium* data, as can be seen from Figure 3 for the glucose, CO_2 and acetate fluxes. The reconstructed model therefore seemed to be inefficient, because it was not able to describe the lower biomass fluxes and higher organic acid fluxes observed for *Salmonella*.

Simulations with the STM_v1.0 model were also carried out for anaerobic conditions (oxygen flux = 0) using the pFBA method and the same objective function (biomass maximization). The simulated fluxes are shown in Figure 4, together with the experimental values for *E. coli*[19] and *S. typhimurium*, for comparison.

The simulated fluxes confirmed the low growth rate observed experimentally for the anaerobic culture. Substantial formate, ethanol, and acetate fluxes were estimated by the simulations, whereas no lactate or CO_2 formation was predicted. The values of the *in silico* and *in vitro* fluxes were significantly different, especially for *Salmonella*, and once again, the model predictions for the anaerobic conditions did not provide an accurate description of cell metabolism.

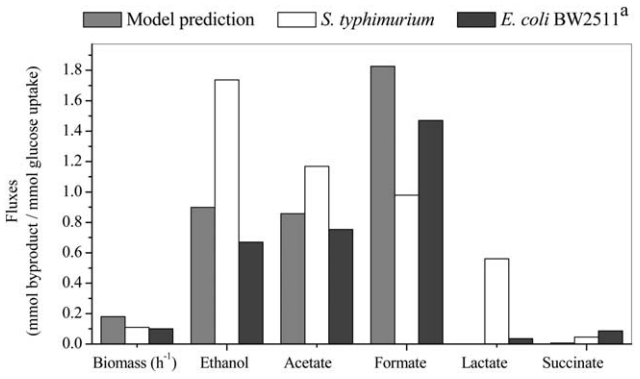

Figure 4. Comparison between experimental data for anaerobic batch cultivation and *in silico* solutions using the experimental GUF value (9.6 mmol g_{DCW}^{-1} h^{-1}), constraining the maximum oxygen uptake rate to zero in the environmental conditions used for the pFBA simulation.

[a]Data from Castaño-Cerezo et al.[19]

Conclusions

From data obtained during *S. typhimurium* cultures under aerobic and anaerobic conditions, using glucose or acetic acid as carbon source, it was possible to map extracellular metabolite formation.

Chemostat cultivations of *S. typhimurium* at various growth rates showed that *Salmonella* cells exhibit a mixed metabolism, with both respiration and fermentation occurring. Acetate is secreted even under completely aerobic conditions and at low specific growth rates, which was not observed for *E. coli* under the same conditions.

Both bacteria are able to assimilate acetate as carbon source. However, it was shown here that the rate of consumption of acetate by *Salmonella* was much lower than reported for *E. coli* strains. This finding suggests that acetate accumulation is a greater obstacle to the establishment of high cell density cultivations of *S. typhimurium*.

During anaerobic growth, *S. typhimurium* produced mainly ethanol, acetate and formate, as also found for *E. coli*. However, *E. coli* showed a greater ability to assimilate glucose.

In silico studies of *S. typhimurium* metabolism were performed using the genome-scale STM_v1.0 metabolic model reconstructed for *S. typhimurium*. This model, which is based on the *E. coli* metabolic network, provided a poor description of the experimental results obtained with *S. typhimurium*. Although *E. coli* and *Salmonella* share the same reactions involved in the central carbon metabolism pathways, these bacteria show distinct regulation mechanisms and reaction kinetics in these pathways.[54] For these reasons, they can exhibit different growth rates under similar cultivation conditions, as well as differences in the capacity to metabolize certain substrates.[46,54]

The results therefore demonstrate that the use of a modified metabolic model originally designed for *E. coli* is not sufficient for description of the central carbon metabolism of *S. typhimurium*. The necessary improvements to the model depend on a better understanding of *S. typhimurium* central carbon metabolism, which could be achieved by a more detailed analysis of intracellular metabolite fluxes provided by ^{13}C metabolic flux analysis (^{13}C MFA).

Once an improved model becomes available, metabolic engineering strategies based on the results of simulations could be used to optimize cell metabolism and drive the carbon flux more efficiently towards biomass formation.

Acknowledgments

Special thanks to Amadeus Azevedo for the HPLC analyses and technical assistance. The authors acknowledge the national funding received from CNPq (Conselho Nacional de Desenvolvimento Científico e Tecnológico, Brazil), the international cooperation project CAPES-FCT (Coordenação de Aperfeiçoamento de Pessoal de Nível Superior/Brazil—Fundação para a Ciência e a Tecnologia/Portugal—Process 315/11), CAPES (Atração de Jovens Talentos—Process 064922/2014-01) and to Fundação para a Ciência e Tecnologia the strategic funding of UID/BIO/04469/2013 unit.

Literature Cited

1. Hegazy WAH, Hensel M. *Salmonella enterica* as a vaccine carrier. *Future Microbiol*. 2012;7:111–127.
2. Jelsbak L, Hartman H, Schroll C, Rosenkrantz JT, Lemire S, Wallrodt I, Thomsen LE, Poolman M, Kilstrup M, Jensen PR, Olsen JE. Identification of metabolic pathways essential for fitness of *Salmonella typhimurium in vivo*. *PloS One*. 2014;9: e101869
3. Majowicz SE, Musto J, Scallan E, Angulo FJ, Kirk M, O'Brien SJ, Jones TF, Fazil A, Hoekstra RM. The global burden of nontyphoidal *Salmonella* gastroenteritis. *Clin Infect Dis*. 2010;50: 882–889.
4. Silva AJ, Zangirolami TC, Novo MTM, Giordano RC, Martins EAL. Live bacterial vaccine vectors: an overview. *Braz J Microbiol*. 2014;45:1117–1129.
5. Carleton HA. Pathogenic bacteria as vaccine vectors: teaching old bugs new tricks. *Yale J Biol Med*. 2010;83:217–222.
6. Chin'ombe N. Recombinant *Salmonella enterica* serovar Typhimurium as a vaccine vector for HIV-1 Gag. *Viruses*. 2013;5: 2062–2078.
7. Gómez-Duarte OG, Bumann D, Meyer TF. The attenuated *Salmonella* vaccine approach for the control of *Helicobacter pylori* related diseases. *Vaccine*. 1999;17:1667–1673.
8. Husseiny MI, Rawson J, Kaye A, Nair I, Todorov I, Hensel M, Kandeel F, Ferreri K. An oral vaccine for type 1 diabetes based on live attenuated *Salmonella*. *Vaccine*. 2014;32:2300–2307.
9. Synnott A, Ohshima K, Nakai Y, Tanji Y. IgA response of BALB/c mice to orally administered *Salmonella typhimurium* flagellin-displaying T2 bacteriophages. *Biotechnol Prog*. 2009; 25:552–558.
10. Hiller J, Franco-Lara E, Weuster-Botz D. Metabolic profiling of *Escherichia coli* cultivations: evaluation of extraction and metabolite analysis procedures. *Biotechnol Lett*. 2007;29:1169–1178.
11. Darji A, Lage S, Garbe AI, Chakraborty T, Weiss S. Oral delivery of DNA vaccines using attenuated *Salmonella typhimurium* as carrier. *FEMS Immunol Med Microbiol*. 2000;27:341–349.
12. Kong W, Clark-Curtiss J, Curtiss IIIR. Utilizing *Salmonella* for antigen delivery: the aims and benefits of bacterial delivered vaccination. *Expert Rev Vaccines*. 2013;12:345–347.
13. Starai VJ, Escalante-Semerena JC. Acetyl-coenzyme A synthetase (AMP forming). *Cell Mol Life Sci*. 2004;61:2020–2030.
14. Starai VJ, Gardner JG, Escalante-Semerena JC. Residue Leu-641 of acetyl-CoA synthetase is critical for the acetylation of residue Lys-609 by the protein acetyltransferase enzyme of *Salmonella enterica*. *J Biol Chem*. 2005;280:26200–26205.
15. Starai VJ, Garrity J, Escalante-Semerena JC. Acetate excretion during growth of *Salmonella enterica* on ethanolamine requires phosphotransacetylase (EutD) activity, and acetate recapture requires acetyl-CoA synthetase (Acs) and phosphotransacetylase (Pta) activities. *Microbiology*. 2005;151:3793–3801.
16. Thao S, Escalante-Semerena JC. Control of protein function by reversible N ε-lysine acetylation in bacteria. *Curr Opin Microbiol*. 2011;14:200–204.

17. Wang Q, Zhang Y, Yang C, Xiong H, Lin Y, Yao J, Li H, Xie L, Zhao W, Yao Y, Ning Z, Zeng R, Xiong Y, Guan K, Zhao S, Zhao GP. Acetylation of metabolic enzymes coordinates carbon source utilization and metabolic flux. *Science*. 2010;327: 1004–1007.
18. Blattner FR, Plunkett G, Bloch CA, Perna NT, Burland V, Riley M, Collado-Vides J, Glasner JD, Rode CK, Mayhew GF, Gregor J, Davis NW, Kirkpatrick HA, Goeden MA, Rose DJ, Mau B, Shao Y. The complete genome sequence of *Escherichia coli* K-12. *Science*. 1997;277:1453–1462.
19. Castaño-Cerezo S, Pastor JM, Renilla S, Bernal V, Iborra JL, Cánovas M. An insight into the role of phosphotransacetylase (pta) and the acetate/acetyl-CoA node in *Escherichia coli*. *Microb Cell Fact*. 2009;8:54
20. De Mey M, Lequeux GJ, Beauprez JJ, Maertens J, Van Horen E, Soetaert WK, Vanrolleghem PA, Vandamme EJ. Comparison of different strategies to reduce acetate formation in *Escherichia coli*. *Biotechnol Prog*. 2007;23:1053–1063.
21. Kleman GL, Strohl WR. Acetate metabolism by *Escherichia coli* in high-cell-density fermentation. *Appl Environ Microbiol*. 1994;60:3952–3958.
22. Oh MK, Rohlin L, Kao KC, Liao JC. Global expression profiling of acetate-grown *Escherichia coli*. *J Biol Chem*. 2002;277: 13175–13183.
23. Paczia N, Nilgen A, Lehmann T, Gätgens J, Wiechert W, Noack S. Extensive exometabolome analysis reveals extended overflow metabolism in various microorganisms. *Microb Cell Fact*. 2012;11:122
24. Andersson C, Hodge D, Berglund KA, Rova U. Effect of different carbon sources on the production of succinic acid using metabolically engineered *Escherichia coli*. *Biotechnol Prog*. 2007; 23:381–388.
25. Wang Q, Ou MS, Kim Y, Ingram LO, Shanmugam KT. Metabolic flux control at the pyruvate node in an anaerobic *Escherichia coli* strain with an active pyruvate dehydrogenase. *Appl Environ Microbiol*. 2010;76:2107–2114.
26. Renilla S, Bernal V, Fuhrer T, Castaño-Cerezo S, Pastor JM, Iborra JL, Sauer U, Cánovas M. Acetate scavenging activity in *Escherichia coli*: interplay of acetyl–CoA synthetase and the PEP–glyoxylate cycle in chemostat cultures. *Appl Microbiol Biotechnol*. 2012;93:2109–2124.
27. Vemuri GN, Altman E, Sangurdekar DP, Khodursky AB, Eiteman MA. Overflow metabolism in *Escherichia coli* during steady-state growth: transcriptional regulation and effect of the redox ratio. *Appl Environ Microbiol*. 2006;72:3653–3661.
28. Xu B, Jahic M, Blomsten G, Enfors SO. Glucose overflow metabolism and mixed-acid fermentation in aerobic large-scale fed-batch processes with *Escherichia coli*. *Appl Microbiol Biotechnol*. 1999;51:564–571.
29. Bernstein HC, Paulson SD, Carlson RP. Synthetic *Escherichia coli* consortia engineered for syntrophy demonstrate enhanced biomass productivity. *J Biotechnol*. 2012;157:159–166.
30. Shiloach J, Fass R. Growing *E. coli* to high cell density—a historical perspective on method development. *Biotechnol Adv*. 2005;23:345–357.
31. Valgepea K, Adamberg K, Nahku R, Lahtvee PJ, Arike L, Vilu R. Systems biology approach reveals that overflow metabolism of acetate in *Escherichia coli* is triggered by carbon catabolite repression of acetyl-CoA synthetase. *BMC Syst Biol*. 2010;4:166
32. AbuOun M, Suthers PF, Jones G, Carter BR, Saunders MP, Maranas CD, Woodward MJ, Anjum MF. Genome scale reconstruction of a Salmonella metabolic model: comparison of similarity and differences with a commensal *Escherichia coli* strain. *J Biol Chem*. 2009;284:29480–29488.
33. McClelland M, Sanderson KE, Spieth J, Clifton SW, Latreille P, Courtney L, Porwollik S, Ali J, Dante M, Du F, Hou S, Layman D, Leonard S, Nguyen C, Scott K, Holmes A, Grewal N, Mulvaney E, Ryan E, Sun H, Florea L, Miller W, Stoneking T, Nhan M, Waterston R, Wilson RK. Complete genome sequence of *Salmonella enterica* serovar Typhimurium LT2. *Nature*. 2001;413:852–856.
34. Götz A, Eylert E, Eisenreich W, Goebel W. Carbon metabolism of enterobacterial human pathogens growing in epithelial colorectal adenocarcinoma (Caco-2) cells. *PLoS One*. 2010;5:e10586
35. Wilson PDG, Wilson DR, Brocklehurst TF, Coleman HP, Mitchell G, Waspe CR, Jukes SA, Robins MM. Batch growth of *Salmonella typhimurium* LT2: stoichiometry and factors leading to cessation of growth. *Int J Food Microbiol*. 2003;89:195–203.
36. du Preez JC, van Rensburg E, Kilian SG. Kinetics of growth and leukotoxin production by *Mannheimia haemolytica* in continuous culture. *J Ind Microbiol Biotechnol*. 2008;35:611–618.
37. Kayser A, Weber J, Hecht V, Rinas U. Metabolic flux analysis of *Escherichia coli* in glucose-limited continuous culture. I. Growth-rate-dependent metabolic efficiency at steady state. *Microbiology*. 2005;151:693–706.
38. Sauer U, Hatzimanikatis V, Hohmann HP, Manneberg M, Van Loon AP, Bailey JE. Physiology and metabolic fluxes of wild-type and riboflavin-producing *Bacillus subtilis*. *Appl Environ Microbiol*. 1996;62:3687–3696.
39. Rocha I, Maia P, Evangelista P, Vilaça P, Soares S, Pinto JP, Nielsen J, Patil KR, Ferreira EC, Rocha M. OptFlux: an open-source software platform for *in silico* metabolic engineering. *BMC Syst Biol*. 2010;4:45.
40. Raman K, Chandra N. Flux balance analysis of biological systems: applications and challenges. *Briefings Bioinf*. 2009;10: 435–449.
41. Chaganti SR, Kim DH, Lalman JA. Flux balance analysis of mixed anaerobic microbial communities: effects of linoleic acid (LA) and pH on biohydrogen production. *Int J Hydrogen Energy*. 2011;36:14141–14152.
42. Senger RS, Papoutsakis ET. Genome-scale model for *Clostridium acetobutylicum*: part I. Metabolic network resolution and analysis. *Biotechnol Bioeng*. 2008;101:1036–1052.
43. Raman K, Rajagopalan P, Chandra N. Flux balance analysis of mycolic acid pathway: targets for anti-tubercular drugs. *PLoS Comput Biol*. 2005;1:e46
44. Shinfuku Y, Sorpitiporn N, Sono M, Furusawa C, Hirasawa T, Shimizu H. Development and experimental verification of a genome-scale metabolic model for *Corynebacterium glutamicum*. *Microb Cell Fact*. 2009;8:43
45. Varma A, Palsson BØ. Stoichiometric flux balance models quantitatively predict growth and metabolic by-product secretion in wild-type *Escherichia coli* W3110. *Appl Environ Microbiol*. 1994;60:3724–3731.
46. Thiele I, Hyduke DR, Steeb B, Fankam G, Allen DK, Bazzani S, Charusanti P, Chen F, Fleming RMT, Hsiung CA, Keersmaecker SCJ, Liao Y, Marchal K, Mo ML, Özdemir E, Raghunathan A, Reed JL, Shin S, Sigurbjörnsdóttir S, Steinmann J, Sudarsan S, Swainston N, Thijs IM, Zengler K, Palsson BØ, Adkins JN, Bumann D. A community effort towards a knowledge-base and mathematical model of the human pathogen *Salmonella typhimurium* LT2. *BMC Syst Biol*. 2011;5:1–9.
47. Horta ACL, Zangirolami TC, Giordano RC, Cruz AJ, Reis GB, Jesus CDF. Supervisory system for bioreactor high cell density cultivations. Brazil: Patent 11008-6, RPI 2115, 2011.
48. Horta ACL, Silva AJ, Sargo CR, Velez AM, Gonzaga MC, Gonçalves VM, Giordano RC, Zangirolami TC. A supervision and control tool based on artificial intelligence for high cell density cultivations. *Braz J Chem Eng*. 2014;31:457–468.
49. Stephanopoulos G, Aristidou AA, Nielsen J. Metabolic Engineering: Principles and Methodologies. San Diego: Academic Press Inc; 1998.
50. Shuler ML, Kargi F. How cells grow (2nd edition). In: Bioprocess Engineering: Basic Concepts. New York: Prentice Hall PTR, Inc.; 2007:155–206.
51. Lewis NE, Hixson KK, Conrad TM, Lerman JA, Charusanti P, Polpitiya AD, Adkins JN, Schramm G, Purvine SO, Lopez-Ferrer D, Weitz KK, Eils R, König R, Smith RD Palsson BØ. Omic data from evolved *E. coli* are consistent with computed optimal growth from genome-scale models. *Mol Syst Biol*. 2010; 6:390
52. Castan A, Enfors SO. Formate accumulation due to DNA release in aerobic cultivations of *Escherichia coli*. *Biotechnol Bioeng*. 2002;77:324–328.
53. Brown SW, Meyer HP, Fiechter A. Continuous production of human leukocyte interferon with *Escherichia coli* and continuous cell lysis in a two stage chemostat. *Appl Microbiol Biotechnol*. 1985;23:5–9.

54. Raghunathan A, Reed J, Shin S, Palsson B, Daefler S. Constraint-based analysis of metabolic capacity of *Salmonella typhimurium* during host-pathogen interaction. *BMC Syst Biol*. 2009;3:38
55. Wendisch VF, Graaf AA, Sahm H, Eikmanns BJ. Quantitative determination of metabolic fluxes during coutilization of two carbon sources: comparative analyses with *Corynebacterium glutamicum* during growth on acetate and/or glucose. *J Bacteriol*. 2000;182:3088–3096.
56. Kakuda H, Hosono K, Ichihara S. Identification and characterization of the AckA (acetate kinase A)-Pta (phosphotransacetylase) operon and complementation analysis of acetate utilization by an AckA-Pta deletion mutant of *Escherichia coli*. *J Biochem*. 1994;116:916–922.
57. Kumari S, Tishel R, Eisenbach M, Wolfe AJ. Cloning, characterization, and functional expression of acs, the gene which encodes acetyl coenzyme A synthetase in *Escherichia coli*. *J Bacteriol*. 1995;177:2878–2886.
58. Castaño-Cerezo S, Bernal V, Röhrig T, Termeer S, Cánovas M. Regulation of acetate metabolism in Escherichia coli BL21 by protein Nε-lysine acetylation. *Appl Microbiol Biotechnol.* 2015:1–13.
59. Kao KC, Yang YL, Boscolo R, Sabatti C, Roychowdhury V, Liao JC. Transcriptome-based determination of multiple transcription regulator activities in *Escherichia coli* by using network component analysis. *Proc Natl Acad Sci USA*. 2004;101:641–646.
60. Kao KC, Tran LM, Liao JC. A global regulatory role of gluconeogenic genes in *Escherichia coli* revealed by transcriptome network analysis. *J Biol Chem*. 2005;280:36079–36087.
61. Chittori S, Savithri HS, Murthy MR. Structural and mechanistic investigations on *Salmonella typhimurium* acetate kinase (AckA): identification of a putative ligand binding pocket at the dimeric interface. *BMC Struct Biol*. 2012;12:24
62. Fox DK, Roseman S. Isolation and characterization of homogeneous acetate kinase from *Salmonella typhimurium* and *Escherichia coli*. *J Biol Chem*. 1986;261:13487–13497.
63. Brown TDK, Jones-Mortimer MC, Kornberg HL. The enzymic interconversion of acetate and acetyl-coenzyme A in *Escherichia coli*. *J Gen Microbiol*. 1977;102:327–336.
64. Liu F, Gu J, Wang X, Zhang XE, Deng J. Acs is essential for propionate utilization in *Escherichia coli*. *Biochem Biophys Res Commun*. 2014;449:272–277.
65. Chan CH, Garrity J, Crosby HA, Escalante -Semerena JC. In *Salmonella enterica*, the sirtuin-dependent protein acylation/deacylation system (SDPADS) maintains energy homeostasis during growth on low concentrations of acetate. *Mol Microbiol*. 2011;80:168–183.
66. Reger AS, Carney JM, Gulick AM. Biochemical and crystallographic analysis of substrate binding and conformational changes in acetyl-CoA synthetase. *Biochemistry*. 2007;46:6536–6546.
67. Andersen KB, von Meyenburg K. Are growth rates of *Escherichia coli* in batch cultures limited by respiration? *J Bacteriol*. 1980;144:114–123.
68. Driessen M, Postma PW, Dam K. Energetics of glucose uptake in *Salmonella typhimurium*. *Arch Microbiol*. 1987;146:358–361.
69. Chen X, Alonso AP, Allen DK, Reed JL, Shachar-Hill Y. Synergy between ^{13}C-metabolic flux analysis and flux balance analysis for understanding metabolic adaption to anaerobiosis in *E. coli*. *Metab Eng*. 2011;13:38–48.

Manuscript received Mar. 16, 2015, and revision received May 20, 2015.